Optical Materials 133 (2022) 112934

Contents lists available at ScienceDirect

Optical Materials

journal homepage: www.elsevier.com/locate/optmat

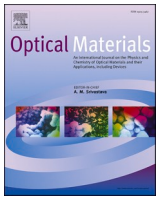

Research Article

Photoluminescence and X-ray induced scintillation in Gd^{3+}-modified fluorophosphate glasses doped with Ce^{3+}

Gustavo Galleani [a,*], Thiago A. Lodi [a], Valmor R. Mastelaro [a], Luiz G. Jacobsohn [b], Andrea S.S. de Camargo [a,**]

[a] São Carlos Institute of Physics, University of São Paulo, São Carlos, SP, Brazil
[b] Department of Materials Science and Engineering, Clemson University, Clemson, SC, USA

ARTICLE INFO

Keywords:
Fluorophosphate glasses
Scintillators
Cerium
Energy transfer

ABSTRACT

In this work, we report the fabrication of Gd^{3+}-modified fluorophosphate glasses doped with Ce^{3+} with the new compositions $50NaPO_3$–$20BaF_2$-(10-x)CaF_2-$20GdF_3$-x$CeCl_3$, x = 0.3; 1; 3 and 5 mol% and their promising features as scintillators. The glasses present high molar density values ($\rho \cong 4$ g cm^{-3}), comparable to that of crystal scintillators, and distinguished optical properties. By UV–visible absorption, photoluminescence emission and excitation, excited state decay curves and radioluminescence measurements, the photophysical properties of the glasses were fully characterized. In addition, x-ray photoelectron spectroscopy (XPS) was employed to confirm the valence state of Ce ions. The results of emission spectra measured in the visible range upon UV excitation together with the excited state lifetime values of Ce^{3+} ($5d \rightarrow 4f$ transition) and Gd^{3+} ($^8S_{7/2} \rightarrow {}^6I_j$ transition) clearly evidence energy transfer (ET) from the latter to the former ion. Though not quantified, the ET favors the fast decaying ($\tau = 24$ ns) efficient emission of Ce^{3+} which makes the materials promising for fast response high energy radiation detectors. The response to X-ray excitation associated with the relatively high molar density of the glasses, indicate the promising application of these glasses for medical diagnosis where, in particular, a fast and intense response under high-energy radiation excitation is crucial.

1. Introduction

A scintillator is a material with the capability to absorb the energy of incoming ionizing radiation and converting it into ultraviolet/visible light photons, via a complex process that includes the excitation and relaxation of electrons in luminescent centers (intrinsic or extrinsic) [1]. Generally, extrinsic scintillation is achieved through doping, *i.e.*, the incorporation of transition metal dopant ions displaying f-d and f-f transitions such as Dy^{3+}, Eu^{3+}, Tb^{3+} and Ce^{3+} [2–4] into a solid-state host matrix. On the other hand, intrinsic scintillation, avails the benefit of molecular groups or defects to be subjected to radiative transitions that do not involve discrete ionic electronic levels [5,6]. In both cases, the resulting photons can be detected by photodiode detectors and photomultiplier tubes (PMTs). Scintillators are important materials in a large range of applications such as medical imaging, nuclear plant safety, radioactive contamination and high-energy and nuclear physics [7–12].

Currently, an extensive diversity of crystalline inorganic and organic scintillating materials are known [9,13]. However, robust inorganic crystals still require costly and time-consuming fabrication methods, resulting in expensive materials with limited shapes and sizes. Organic crystals, in contrast, can be produced in much larger sizes and volumes but have low density and thus lower detection sensitivity, in addition to presenting the inability to identify the radioactive source material (*i.e.*, energy resolution). As an alternative to these drawbacks, increasing interest has been demonstrated onto glass scintillators [14] owing to the considerable extent of possible chemical composition range and good formability. Glasses can be produced in a suitable, simpler and more economical fashion than crystalline materials resulting in optically active materials with vast variety of shapes, sizes, compositions, homogeneity, and low optical scattering. Despite of that, an obstacle for the glass scintillators is the lower density exhibited by conventional oxide glass compositions as compared to crystals. One strategy to overcome this disadvantage is to use chemical elements with high

* Corresponding author.
** Corresponding author.
E-mail addresses: gugalleani@yahoo.com.br (G. Galleani), andreasc@ifsc.usp.br (A.S.S. de Camargo).

https://doi.org/10.1016/j.optmat.2022.112934
Received 17 August 2022; Received in revised form 23 August 2022; Accepted 25 August 2022
Available online 9 September 2022

atomic numbers as network modifiers [15–17]. Various works propose the use of Gd to increase the glass density and enhance the ionizing radiation absorption coefficient. Also, Gd^{3+} ions enable efficient absorption of the high energy radiation and energy transfer to visible emitting centers [18,19].

Currently, there are only a few reports in the literature on the use of fluorophosphate glasses as scintillators [20,21] most of them are focused on the use of oxide glasses [14,22–25]. Fluorophosphate glass compositions are promising because they can combine desirable properties from both fluoride and oxide glassy components. On one hand, fluorides exhibit wider transmission range from the ultraviolet to the infrared region [26], higher radiation resistance to high energy photons [27], and the possibility of a lower vibrational energy environment for rare earth active ions, favoring radiative emissions. On the other hand, the oxide (phosphate) offers network structure stabilization by oxygen species and can also favor the incorporation of higher amounts of dopant ions [28].

In the case of scintillators, requiring fast response, i.e., for medical imaging as in computed tomography, appropriate matching between emission wavelengths and the camera's response (typically 300–400 nm for PMTs) is required and, for that purpose, several Ce^{3+} activated materials have been investigated and proposed [28–34]. However, some chemical compositions of glasses can interfere with the valence state of Ce and, as a consequence, its emission efficiency. The presence of Ce^{4+} can adversely affect the characteristic Ce^{3+} luminescence [3,35,36] and it is known that when the optical basicity of the medium is increased, the oxidation of Ce^{3+} to Ce^{4+} is favored [37]. This drawback can be overcome in more acidic glass compositions, as it is the case of fluorophosphates.

Despite these promising characteristics, to this date only limited effort has been committed to the investigation of Ce^{3+}-Gd^{3+} co-doped fluorophosphate glasses, where Gd^{3+} ions are mainly used as a dopant, and not in structure modifying quantities. For the past ten years, various fluorophosphate glass compositions have been explored by our research group for applications ranging from laser active media to optical thermometers. In the present work, we report the fabrication and characterization of new Ce^{3+} doped glass compositions based on the $NaPO_3$–BaF_2–CaF_2-GdF_3 system with fairly high GdF_3 content (20 mol %). In light of the promising application as scintillators, special attention was given to the possible energy transfer from Gd^{3+} to Ce^{3+} ions and to the maintenance of Ce^{3+} valence state through X-ray photoelectron spectroscopy (XPS) investigations.

2. Experimental

Bulk glass synthesis: Cerium-doped fluorophosphate glasses in the compositional system $50NaPO_3$–$20BaF_2$-$(10\text{-}x)CaF_2$-$20GdF_3$-$xCeCl_3$ with x = 0.3; 1; 3 and 5 mol% were prepared by the conventional melt quenching technique. Starting materials were $NaPO_3$ (Sigma, 99.9%), CaF_2 (Alfa Aesar, 99.95%), BaF_2 (Alfa Aesar, 99.9%), $CeCl_3.7H_2O$ (Sigma, 99.9%) and GdF_3. The GdF_3 precursor was prepared by heating Gd_2O_3 (Sigma, 99.9%) with an excess of $NH_4H_2F_4$ (Synth, 98%) in a platinum tube at 300 °C in air during 1 h [38]. 6 g bulk glasses were obtained by mixing and heating the components with molar compositions detailed in Table 1 in a capped platinum crucible and melted at 800 °C in a conventional furnace in air atmosphere. The density values were measured using a home-made apparatus according to the Archimedes principle, using distilled water as the immersion liquid, at room temperature.

Table 1
Nominal composition (mol %) and density of the investigated glasses.

Glass sample	$NaPO_3$	GdF_3	CaF_2	BaF_2	$CeCl_3$	ρ (g/cm^3) ±0.4
NPGF	50	20	10	20	0	4.2
NPGF_0.3Ce	50	20	9.7	20	0.3	4.1
NPGF_1Ce	50	20	9	20	1	4.1
NPGF_3Ce	50	20	7	20	3	4.0
NPGF_5Ce	50	20	5	20	5	4.0

Glass samples characterization: Absorption spectra of polished samples with approximately 2 mm thickness were measured using a Cary 500 (Varian) double-beam spectrometer in the range 200–600 nm. Visible photoluminescence emission (PL) and excitation (PLE) spectra were measured using a Horiba Jobin Yvon Fluorolog spectrofluorimeter model FL3-221 equipped with a Xe lamp. The emission spectra were measured with excitation at 273 nm while the excitation spectra were collected by monitoring the Ce^{3+} emission at 350 nm. The luminescence decay curves of the Gd^{3+} emission ($^8S_{3/2} \rightarrow {}^6P_{7/2}$, 311 nm) were measured with excitation from a pulsed Xe lamp at 273 nm, while the luminescence decay curves of Ce^{3+} were measured at 350 nm using the time-correlated single-photon counting (TCSPC) mode, with excitation at 289 nm from a Delta Diode coupled to the fluorimeter. The luminescence signals were analyzed by a double monochromator configuration with 1 nm slits, and collected by a PPD visible detector. Radioluminescence (RL) measurements were done in a spectrofluorometer model Freiberg Instruments Lexsyg Research, equipped with a Varian Medical Systems VF50J X-ray tube operating at 40 kV and 1 mA, with a tungsten target. The signal was collected by an Andor Technology Shamrock 163 spectrograph coupled to a CCD camera model Andor Technology DU920P-BU Newton, kept at −80 °C.

XPS analysis was performed in ultrahigh vacuum (low 10^{-9} Pa range) using a ScientaOmicron ESCA + spectrometer equipped with a high-performance hemispheric analyzer (EA 125), adjusted to a pass energy of 50 eV. Monochromatic Al Kα ($h\nu = 1486.6$ eV) radiation was used as the excitation source at 11 kV and 14 mA. The analysis was done in powder samples fixed on a steel holder with a carbon double-face adhesive tape. An analyzer pass energy of 20 eV was used to obtain the high-resolution spectra. The binding energies were referenced to the carbon 1s line set at 284.5 eV. A mixed Gaussian/Lorentzian function was used to fit the spectra of Ce 3d using the CASA XPS software.

3. Results and discussion

Photographs of the Ce^{3+}-doped NPGF glass samples under ambient light and under 273 nm excitation are shown in Fig. 1. Homogeneous, non-hygroscopic, and visually transparent colorless glasses were obtained.

As depicted in Table 1, the undoped glass has a volumetric density of 4.2 g/cm^{-3} and the addition of $CeCl_3$ does not change this value significantly. The density values of all samples are superior to that of commercially available Ce^{3+}-doped ^{6}Li silicate glass, GS20® (2.5 g/cm^3) [39] and NaI:Tl crystal (3.67 g/cm^3) [40], suggesting the appropriateness of these glasses for the intended application. The NPGF glass also exhibits higher volumetric density values than the fluorophosphate glass containing Gd (ρ = 3.70 g/cm^3), previously reported by Yao et al. [41].

The absorption spectra in the range 200–600 nm of the doped glasses and the reference NPGF host glass are shown in Fig. 2. For the NPGF glass, the UV edge is around 310 nm and the characteristic absorptions bands of Gd^{3+}, observed at 245, 251, 273, 305 and 311 nm, are assigned to transitions from the ground state $^8S_{7/2}$ to the excited states ^6I_j and ^6P_j, respectively. In the case of cerium doped NPGF glasses, a strong absorption is observed in the UV region, which is red-shifted with the increase of cerium content. The absorption is associated with the $4f$–$5d_j$ transitions of Ce^{3+} as reported in the literature for other glass systems [34,42,43]. This observation has also been reported for other similar glasses, as a consequence of the energy shift of the 4f-5d transition with the increase of cerium content [44].

The chemical state of cerium ions in the NPGF glass powders with different cerium contents was investigated by XPS, and the Ce 3d spectra are shown in Fig. 3, together with the curve fitting. Two components were used to fit the spectra for Ce $3d_{5/2}$ and another two for Ce $3d_{3/2}$

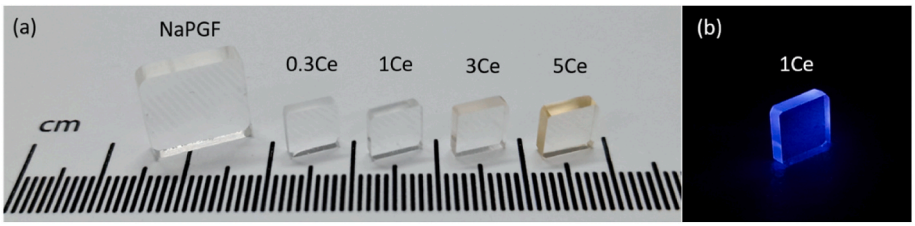

Fig. 1. Photographs (a) of the Cerium doped NPGF glasses with different Ce^{3+} dopant concentrations under ambient light, and (b) of the representative NPGF_1Ce glass under UV (273 nm) excitation.

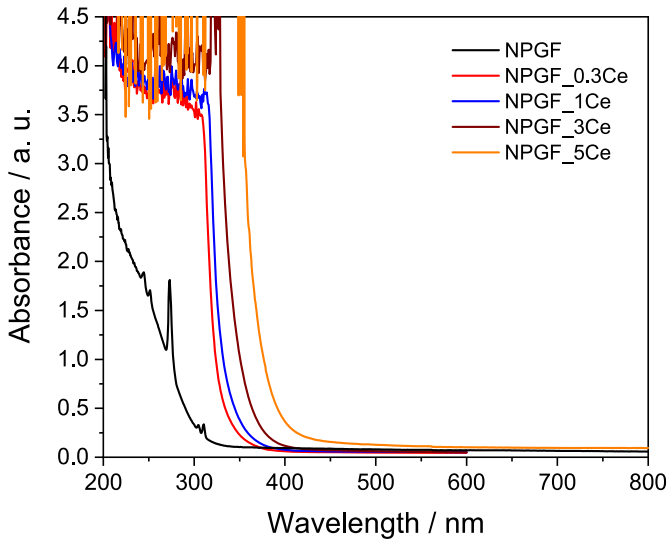

Fig. 2. Absorption spectra measured for the host glass (NPGF) and for the Ce^{3+} containing NPGF glasses with ~2 mm thickness.

peaks, located at 883.1 eV, 886.5 eV and at 901.3 eV, 905.4 eV, respectively. These binding energies are characteristic of Ce^{3+} species [23].

In the case of the presence of Ce^{4+}, a third peak located at ~916 eV in conjunction to three satellites would have been expected, however, it has not been detected in any of the glasses. This result indicates that cerium ions are predominantly present as Ce^{3+}. Mixed fluorophosphate glasses have lower basicity compared to pure oxide glasses, and the Ce^{4+}/Ce^{3+} redox stability may decrease with the increase in acidity of the glass, allowing to shift the equilibrium for active Ce^{3+} ions in our glasses [3].

Fig. 4 shows the PLE and PL spectra of the undoped and Ce^{3+}-doped NPGF glasses. For the undoped glass, sharp excitation lines attributed to Gd^{3+} transitions are observed at 247 nm ($^8S_{7/2} \rightarrow {}^6D_{5/2}$), 253 nm ($^8S_{7/2} \rightarrow {}^6D_{9/2}$), 273 nm ($^8S_{7/2} \rightarrow {}^6I_{5/2}$), 275 nm ($^8S_{7/2} \rightarrow {}^6I_{7/2}$) and 278 nm ($^8S_{7/2} \rightarrow {}^6I_{9/2}$) by monitoring the ion's PL emission at 311 nm. For the Ce^{3+} doped NPGF glasses, a broad excitation band around 320 nm ($4f \rightarrow 5d_j$ transitions), is observed by monitoring the emission of Ce^{3+} at 350 nm. This excitation band is red-shifted with increasing Ce^{3+} concentration, similarly to what was observed for the absorption spectra and also reported in the literature [20].

The PL emission spectra were all measured with excitation at 273 nm, in order to probe the energy transfer (ET) from Gd^{3+} to Ce^{3+}, although cerium can also be weakly, directly excited at this wavelength.

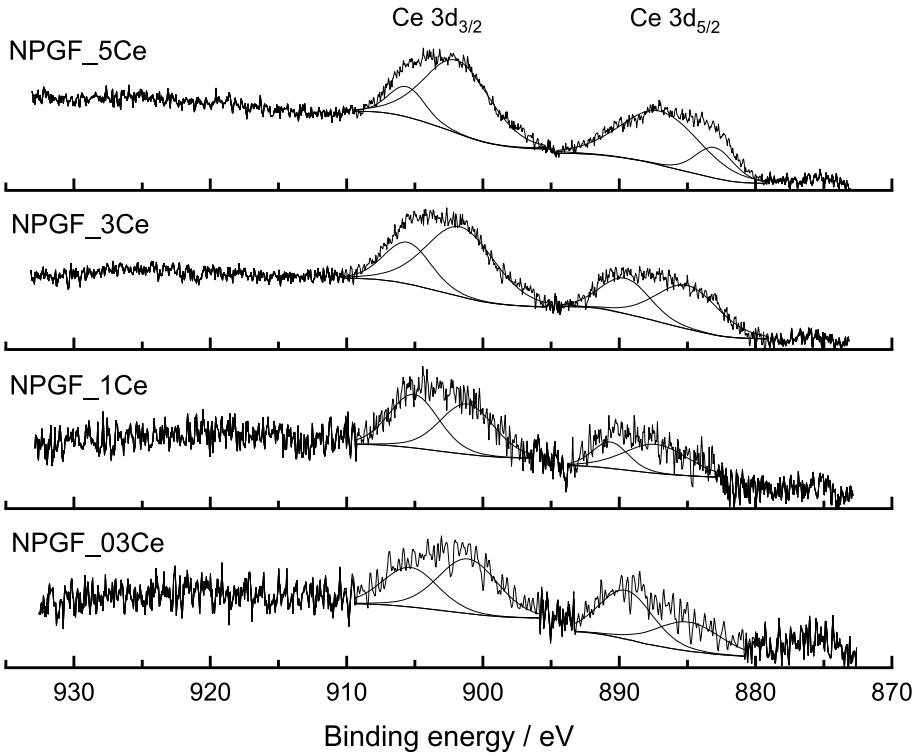

Fig. 3. XPS spectra of Ce. The 3d spin orbit doublet of Ce and the results obtained from the peak fitting procedure are shown in the range 910–880 eV.

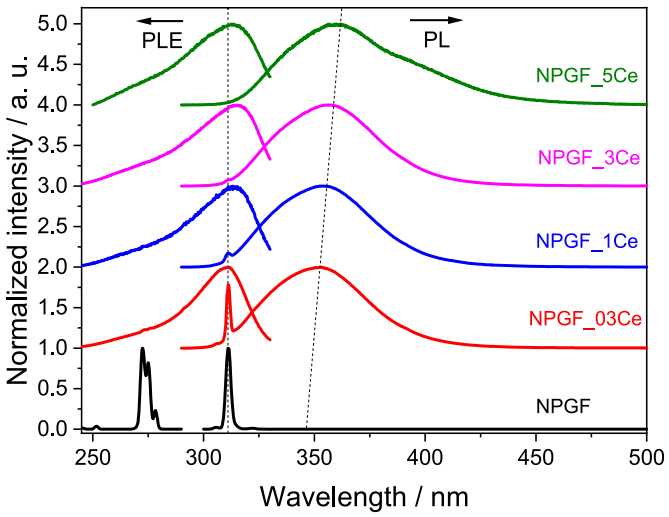

Fig. 4. Left: Normalized photoluminescence excitation (PLE) spectra monitoring the emission at 350 nm (Ce^{3+}-doped samples, $^8S_{3/2} \rightarrow {}^2F_{5/2}$) or at 311 nm (undoped sample, $^6P_j \rightarrow {}^8S_{7/2}$). Right: Normalized emission (PL) spectra with excitation at 273 nm, measured for Ce doped and undoped NPGF glasses.

Besides the evident $Gd^{3+} \rightarrow Ce^{3+}$ energy transfer, that yield the broad PL emission of Ce^{3+} around ~355 nm ($5d_j$-$4f$ transitions) [49–54], the Gd^{3+} ions can also emit independently at 311 nm ($^6P_j \rightarrow {}^8S_{7/2}$ transition), as evidenced in the spectra of NPGF_03Ce and NPGF_1Ce samples. However, as the dopant concentration increases from 1 to 5 mol%, the Gd^{3+} emission is masked by the overlap with the more intense Ce^{3+} emission. Although we have not studied the ET from a quantitative point of view (beyond the intent of this work) there is also the plausible additional possibility that the increase in acceptor Ce^{3+} ions imposes a decreased emission intensity of the donor Gd^{3+} ions. The occurrence of such $Gd^{3+} \rightarrow Ce^{3+}$ ET is well documented in the literature [19,45–47]. Provided that there is appropriate distance between donor and acceptor ions, a Gd^{3+} ion excited to the ^6Ij states relaxes non-radiatively to its $^6P_{7/2}$ state from which it can resonantly and non-radiatively transfer to the 5d levels of Ce^{3+}, or emit at 311 nm.

Considering the broadband emission of Ce^{3+}, a red-shift is also observed with the increase in the dopant concentration. The center wavelengths are in agreement with those reported for pure phosphate glass (~350–450 nm) and pure fluoride glass (~300–350 nm) [48,49]. The inhomogeneous broadening of the emission band occurs due to the fact that the luminescence arises from non-shielded 5d orbitals strongly susceptible to the strength of the ligand field, in addition to the disordered nature of the glass network.

The emission decay curves of the Ce^{3+}-doped glasses were recorded monitoring the emission at 350 nm, upon excitation at 289 nm by a fast pulsing delta diode and are presented in Fig. 5(a). These curves were fitted using a double-exponential function and include two exponential terms, an ultrafast decay time τ_1 and a fast decay time τ_2, as listed in Table 2. While τ_1 is probably associated to the emission quenching via radiative self-absorption or non-radiative migration to neighboring excited Ce^{3+} ions followed by losses to defects [50] τ_2 is assigned to the decay time of Ce^{3+} allowed $5d \rightarrow 4f$ transition [50,51] as compared to other reported Ce^{3+} doped oxyfluoride glasses [30,31,52].

A more reliable evaluation of the presence of donor → acceptor ET is provided by the measurement of the donor's excited state lifetime. Fig. 5 (b) shows the decay curves for the Gd^{3+}:$^6P_j \rightarrow {}^8S_{7/2}$ (311 nm) emission as a function of the cerium concentration in the studied glasses. With the increase of the dopant concentration, the decay times decrease from 5.8 ms (NPGF) to 0.19 ms (NPGF_5Ce) and the curves become strongly non-exponential due to the additional non-radiative decay channel, which corroborates the previous findings. Considering that the vibrational structure of the samples is on average the same, a rough estimation of the energy transfer efficiency can be made by taking the ratio of Gd^{3+} lifetime values in the Ce^{3+}-doped and undoped samples i.e. 83 – 96% (for samples doped with 0.3–5 mol%).

The X-ray induced scintillation spectra are presented in Fig. 6. The spectra of the Ce-doped glasses are dominated by a broad band centered at ~350 nm that shifts to longer wavelengths upon increasing Ce^{3+} doping concentration, in agreement with the PL results. The Gd^{3+} emission at 311 nm was also observed for the undoped NPGF glass and for the lowest Ce^{3+} content glass sample (NPGF_03Ce). The scintillation process is complex, but in general terms, it can be simplified in three steps: (1) the high-energy photon interacts with the heavy atoms through the photoelectric effect and inelastic Compton scattering eject hot electrons; (2) electrons and holes migrate through the structure and eventually become thermalized, and (3) the emission center captures a hot electron in an excited state and ideally the electron-hole recombination occurs through a radiative process or the energy is lost non-radiatively by heat [45]. With the increase of Ce^{3+} content in the glasses, a decrease of the Ce^{3+} emission intensity is observed. This effect can be explained by the concentration quenching effect together with increasing of self-absorption as observed in Fig. 5(b), where part of the emitted light is in the range of 0% transmission of the glass. The highest scintillation intensity emission was found for the glass samples with Ce

Table 2
Ce^{3+} excited state decay times in the investigated glasses.

Glass sample	τ_1 (ns)	τ_2 (ns)
NPGF_0.3Ce	5.15	24.06
NPGF_1Ce	5.58	24.35
NPGF_3Ce	5.98	23.82
NPGF_5Ce	7.23	22.10

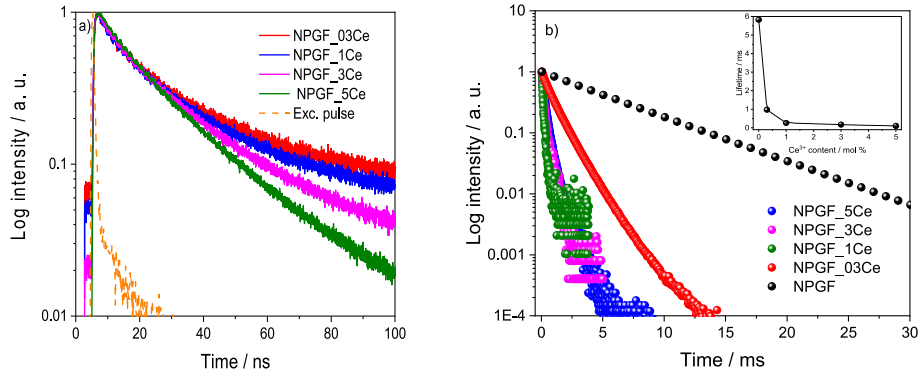

Fig. 5. Photoluminescence decay curves of Ce^{3+} doped and undoped NPGF glasses. (a) Ce^{3+}:$5d \rightarrow 4f$ ($\lambda_{exc} = 289$ nm e $\lambda_{em} = 350$ nm) and (b) Gd^{3+}:$^6P_J \rightarrow {}^8S_{7/2}$ ($\lambda_{exc} = 273$ nm e $\lambda_{em} = 311$ nm).

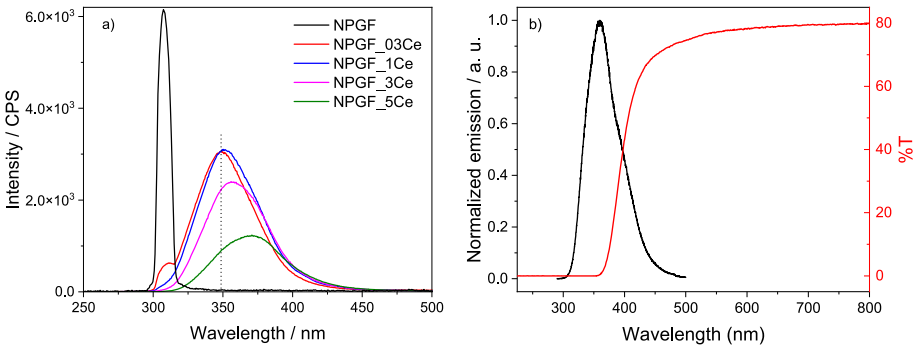

Fig. 6. (a) X-ray induced scintillation spectra of Ce^{3+} doped and undoped NPGF glasses; (b) transmission and emission spectra of the representative NPGF_5Ce sample.

levels within 0.3–1 mol% Ce^{3+}.

The integrated scintillation response of the NPGF_1Ce glass was evaluated in comparison to that of the commercial BGO crystalline (Supporting information, Fig. S1) under the same experimental conditions. The response of the glass is about 7% of that of the powder.

4. Conclusions

Fluorophosphate glasses in the compositional system $NaPO_3$–BaF_2–CaF_2-GdF_3-$CeCl_3$ were prepared through the melt quenching technique with high stability and very good optical quality for scintillating purposes. When compared with commercially available Ce^{3+} glass scintillators, they presented higher molar density values. The conversion of UV and X-ray photons into visible light and the cerium oxidation states were evaluated, and the presence of sole, or at least predominant, trivalent state was verified. The PL excitation and emission, the radioluminescence, and the excited state decay times were evaluated for Gd^{3+} and Ce^{3+}, as a function of the Ce^{3+} dopant content. The origin of the UV to visible energy conversion is mainly attributed to the excitation of the Gd^{3+} ions by ultraviolet light to the level ^6Ij, followed by resonant radiative and non-radiative energy transfer to the 5d levels of Ce^{3+}. The decrease of Gd^{3+}:^6P_j decay times with increasing Ce^{3+} concentration gives clear proof of that. The results of this study give evidence that the Ce^{3+} doped NPGF fluorophosphate glasses can be considered potential candidates for glass scintillators, particularly in applications that require fast time (ns) response.

CRediT authorship contribution statement

Gustavo Galleani: Conceptualization, Methodology, Investigation, Data curation, Writing – original draft, preparation. **Thiago A. Lodi:** Investigation, Data curation, Formal analysis, Writing – review & editing. **Valmor R. Mastelaro:** Data curation, Writing – review & editing. **Luiz G. Jacobsohn:** Data curation, Writing – review & editing. **Andrea S.S. de Camargo:** Conceptualization, Writing – review & editing, Supervision.

Declaration of competing interest

The authors declare that they have no known competing financial interests or personal relationships that could have appeared to influence the work reported in this paper.

Data availability

Data will be made available on request.

Acknowledgments

Authors would like to acknowledge the Brazilian funding agencies FAPESP - Fundação de Amparo à Pesquisa do Estado de São Paulo (Project N. 2013/07793–6 and N. 2013/07296-2, CEPID programs); CAPES - Coordenação de Aperfeiçoamento de Pessoal de Nível Superior; CNPq - Conselho Nacional de Desenvolvimento Científico e Tecnológico (Universal project 130562/2018–1). GG personally acknowledges funding by FAPESP, (Postdoctoral grant number 2018/03931–9). L.G. Jacobsohn's contribution was supported by the National Science Foundation under Grant No. 1653016.

Appendix A. Supplementary data

Supplementary data to this article can be found online at https://doi.org/10.1016/j.optmat.2022.112934.

References

[1] M.J. Weber, Inorganic scintillators: today and tomorrow, J. Lumin. 100 (2002), https://doi.org/10.1016/S0022-2313(02)00423-4.
[2] M.J. Weber, Inorganic scintillators: today and tomorrow, J. Lumin. 100 (2002) 35–45, https://doi.org/10.1016/S0022-2313(02)00423-4.
[3] A.D. Sontakke, J. Ueda, J. Xu, K. Asami, M. Katayama, Y. Inada, S. Tanabe, A comparison on Ce3+ luminescence in borate glass and YAG ceramic: understanding the role of host's characteristics, J. Phys. Chem. C 120 (2016) 17683–17691, https://doi.org/10.1021/acs.jpcc.6b04159.
[4] I.C. Pinto, G. Galleani, L.G. Jacobsohn, Y. Ledemi, Y. Messaddeq, A.S.S. de Camargo, Fluorophosphate glasses doped with Eu3+ and Dy3+ for X-ray radiography, J. Alloys Compd. 863 (2021), 158382, https://doi.org/10.1016/j.jallcom.2020.158382.
[5] P.R. Menge, G. Gautier, A. Iltis, C. Rozsa, V. Solovyev, Performance of large lanthanum bromide scintillators, nuclear Instruments and methods in physics research, section A: accelerators, spectrometers, Detect. Assoc. Equipment. (2007) 579, https://doi.org/10.1016/j.nima.2007.04.002.
[6] M. Moszyński, M. Balcerzyk, W. Czarnacki, M. Kapusta, W. Klamra, A. Syntfeld, M. Szawlowski, Intrinsic energy resolution and light yield nonproportionality of BGO, IEEE Trans. Nucl. Sci. (2004), https://doi.org/10.1109/TNS.2004.829491.
[7] T. Ludziejewski, K. Moszyńska, M. Moszyński, D. Wolski, W. Klamra, L.O. Norlin, E. Devitsin, V. Kozlov, Advantages and limitations of LSO scintillator in nuclear physics experiments, IEEE Trans. Nucl. Sci. 42 (1995), https://doi.org/10.1109/23.467826.
[8] S.K. Gupta, Y. Mao, Recent advances, challenges, and opportunities of inorganic nanoscintillators, Front. Optoelectron. 13 (2020), https://doi.org/10.1007/s12200-020-1003-5.
[9] T. Yanagida, Inorganic scintillating materials and scintillation detectors, Proc. Jpn. Acad. Ser. B Phys. Biol. Sci. 94 (2018), https://doi.org/10.2183/pjab.94.007.
[10] B.C. Grabmaier, Crystal scintillators, IEEE Trans. Nucl. Sci. 31 (1984), https://doi.org/10.1109/TNS.1984.4333280.
[11] M. Nikl, Scintillation detectors for x-rays, Meas. Sci. Technol. 17 (2006), https://doi.org/10.1088/0957-0233/17/4/R01. R37–R54.
[12] M. Nikl, A. Yoshikawa, Recent R&D trends in inorganic single-crystal scintillator materials for radiation detection, Adv. Opt. Mater. 3 (2015), https://doi.org/10.1002/adom.201400571.
[13] F.D. Brooks, Development of organic scintillators, Nucl. Instrum. Methods 162 (1979), https://doi.org/10.1016/0029-554X(79)90729-8.
[14] T.A. Lodi, J.F.M. dos Santos, G. Galleani, L.G. Jacobsohn, T. Catunda, A.S.S. de Camargo, Promising Tb3+-doped gallium tungsten-phosphate glass scintillator:

spectroscopy, energy transfer and UV/X-ray sensing, J. Alloys Compd. 904 (2022), 164016, https://doi.org/10.1016/J.JALLCOM.2022.164016.
[15] E. Auffray, D. Bouttet, I. Dafinei, J. Fay, P. Lecoq, J.A. Mares, M. Martini, G. Mazé, F. Meinardi, B. Moine, M. Nikl, C. Pedrini, M. Poulain, M. Schneegans, S. Tavernier, A. Vedda, Cerium doped heavy metal fluoride glasses, a possible alternative for electromagnetic calorimetry, Nucl. Instrum. Methods Phys. Res. Sect. A Accel. Spectrom. Detect. Assoc. Equip. 380 (1996) 524–536, https://doi.org/10.1016/0168-9002(96)00717-6.
[16] C. Mugoni, C. Gatto, A. Pla-Dalmau, C. Siligardi, Structure and luminescence properties of Dy2O3 doped bismuth-borate glasses, J. Non-Cryst. Solids 471 (2017), https://doi.org/10.1016/j.jnoncrysol.2017.06.009.
[17] J. Park, H.J. Kim, S. Kim, J.K. Cheon, J. Kaewkhao, P. Limsuwan, S. Insiripong, X-ray and proton luminescences of bismuth-borate glasses, J. Kor. Phys. Soc. 59 (2011), https://doi.org/10.3938/jkps.59.657.
[18] J.H. Rao, Y.X. Yang, S.L. Yuan, J.B. Zhang, G.R. Chen, S. Baccaro, A. Cecilia, M. Nikl, Effects of Gd3+-Tb3+ energy transfer and Tb3+ self-sensitization on luminescent properties of Tb3+-doped heavy germanate glasses, Gongneng Cailiao/J. Function. Mater. 36 (2005).
[19] D. Shiratori, D. Nakauchi, T. Kato, N. Kawaguchi, T. Yanagida, X-ray-induced scintillation via energy transfer from Gd3+ to Ce3+ in silicate glasses composed of heavy elements, Sensor. Mater. 32 (2020), https://doi.org/10.18494/SAM.2020.2740.
[20] Y. Yao, L. Liu, Y. Zhang, D. Chen, Y. Fang, G. Zhao, Optical properties of Ce3+ doped fluorophosphates scintillation glasses, Opt. Mater. 51 (2016) 94–97, https://doi.org/10.1016/j.optmat.2015.11.026.
[21] I.C. Pinto, G. Galleani, L.G. Jacobsohn, Y. Ledemi, Y. Messaddeq, A.S.S. de Camargo, Fluorophosphate glasses doped with Eu3+ and Dy3+ for X-ray radiography, J. Alloys Compd. 863 (2021), 158382, https://doi.org/10.1016/j.jallcom.2020.158382.
[22] L. Pan, J.K.M.F. Daguano, N.M. Trindade, M. Cerruti, E.D. Zanotto, L.G. Jacobsohn, Scintillation, luminescence and optical properties of Ce-Doped borosilicate glasses, Opt. Mater. 104 (2020), https://doi.org/10.1016/j.optmat.2020.109847.
[23] J. Fu, M. Kobayashi, S. Sugimoto, J.M. Parker, Eu3+-activated heavy scintillating glasses, Mater. Res. Bull. 43 (2008) 1502–1508, https://doi.org/10.1016/j.materresbull.2007.06.024.
[24] M. Ishii, Y. Kuwano, T. Asai, S. Asaba, M. Kawamura, N. Senguttuvan, T. Hayashi, M. Kobayashi, M. Nikl, S. Hosoya, K. Sakai, T. Adachi, T. Oku, H.M. Shimizu, Boron based oxide scintillation glass for neutron detection, in: Nuclear Instruments and Methods in Physics Research, Section A: Accelerators, Spectrometers, Detectors and Associated Equipment, 2005, https://doi.org/10.1016/j.nima.2004.08.027.
[25] S.C. Lü, S.F. Zhou, J.Z. Tang, P. Liu, Research progress in development of glass scintillator, Guangzi Xuebao/Acta Photonica Sinica. 48 (2019), https://doi.org/10.3788/gzxb20194811.1148011.
[26] D. Ehrt, REVIEW: phosphate and fluoride phosphate optical glasses — properties, structure and applications, Physics and Chemistry of Glasses, Eur. J. Glass Sci. Technol. Part B. 56 (2015) 217–234, https://doi.org/10.13036/17533562.56.6.217.
[27] X. Zou, H. Toratani, Radiation resistance of fluorophosphate glasses for high performance optical fiber in the ultraviolet region, J. Appl. Phys. 81 (1997) 3354–3362, https://doi.org/10.1063/1.365029.
[28] Y. Fujimoto, T. Yanagida, N. Kawaguchi, S. Kurosawa, K. Fukuda, D. Totsuka, K. Watanabe, A. Yamazaki, Y. Yokota, A. Yoshikawa, Characterizations of Ce3+-doped CaB2O4 crystalline scintillator, Cryst. Growth Des. 12 (2012) 142–146, https://doi.org/10.1021/cg200885h.
[29] Q. Wang, B. Yang, Y. Zhang, H. Xia, T. Zhao, H. Jiang, High light yield Ce3+-doped dense scintillating glasses, J. Alloys Compd. 581 (2013) 801–804, https://doi.org/10.1016/j.jallcom.2013.07.181.
[30] Y. Du, S. Han, Y. Zou, J. Yuan, C. Shao, X. Jiang, D. Chen, Luminescence properties of Ce3+-doped oxyfluoride aluminosilicate glass and glass ceramics, Opt. Mater. 89 (2019) 243–249, https://doi.org/10.1016/j.optmat.2019.01.018.
[31] Q. Wang, S. Ouyang, W. Zhang, B. Yang, Y. Zhang, H. Xia, Luminescent properties of Ce3+-doped transparent oxyfluoride glass ceramics containing BaGdF5 nanocrystals, J. Rare Earths 33 (2015) 13–19, https://doi.org/10.1016/S1002-0721(14)60376-8.
[32] W. Chewpraditkul, X. He, D. Chen, Y. Shen, Q. Sheng, B. Yu, M. Nikl, R. Kucerkova, A. Beitlerova, C. Wanarak, A. Phunpueok, Luminescence and scintillation of Ce3+-doped oxide glass with high Gd2O3 concentration, Phys. Status Solidi 208 (2011) 2830–2832, https://doi.org/10.1002/pssa.201127365.
[33] M.W. Kielty, M. Dettmann, V. Herrig, M.G. Chapman, M.R. Marchewka, A. A. Trofimov, U. Akgun, L.G. Jacobsohn, Investigation of Ce3 + luminescence in borate-rich borosilicate glasses, J. Non-Cryst. Solids 471 (2017) 357–361, https://doi.org/10.1016/j.jnoncrysol.2017.06.022.
[34] M.W. Kielty, L. Pan, M.A. Dettmann, V. Herrig, U. Akgun, L.G. Jacobsohn, Luminescence of Ce-doped aluminophosphate glasses, J. Mater. Sci. Mater. Electron. 30 (2019), https://doi.org/10.1007/s10854-019-01301-4.
[35] C. Canevali, M. Mattoni, F. Morazzoni, R. Scotti, M. Casu, A. Musinu, R. Krsmanovic, S. Polizzi, A. Speghini, M. Bettinelli, Stability of luminescent trivalent cerium in silica host glasses modified by boron and phosphorus, J. Am. Chem. Soc. 127 (2005), https://doi.org/10.1021/ja052502o.
[36] A. Vedda, N. Chiodini, D. di Martino, M. Fasoli, F. Morazzoni, F. Moretti, R. Scotti, G. Spinolo, A. Baraldi, R. Capelletti, M. Mazzera, M. Nikl, Insights into microstructural features governing Ce3+ luminescence efficiency in sol-gel silica glasses, Chem. Mater. 18 (2006), https://doi.org/10.1021/cm0617541.
[37] A. Herrmann, H.A. Othman, A.A. Assadi, M. Tiegel, S. Kuhn, C. Rüssel, Spectroscopic properties of cerium-doped aluminosilicate glasses, Opt. Mater. Express (2015) 5, https://doi.org/10.1364/ome.5.000720.
[38] M. Poulain, A. Soufiane, Y. Messaddeq, M.A. Aegerter, Fluoride glasses : synthesis and properties, Braz. J. Phys. 22 (1992) 205–217.
[39] C.W.E, van E. Delft, Inorganic scintillators in medical imaging, Phys. Med. Biol. 85 (2002), https://doi.org/10.1016/S0168-9002(03)01542-0. R85–R106.
[40] Y. Zou, W. Zhang, C. Li, Y. Liu, H. Luo, Construction and test of a single sphere neutron spectrometer based on pairs of 6Li-and 7Li-glass scintillators, Radiat. Meas. 127 (2019), 106148, https://doi.org/10.1016/j.radmeas.2019.106148.
[41] Y. Yao, L. Liu, Y. Zhang, D. Chen, Y. Fang, G. Zhao, Optical properties of Ce3+ doped fluorophosphates scintillation glasses, Opt. Mater. 51 (2016) 94–97, https://doi.org/10.1016/j.optmat.2015.11.026.
[42] M. Martini, F. Meinardi, A. Vedda, I. Dafinei, P. Lecoq, M. Nikl, Ce doped hafniate scintillating glasses: thermall stimulated luminescence and photoluminescence, Nucl. Instrum. Methods Phys. Res. B 116 (1996) 116–120, https://doi.org/10.1016/0168-583X(96)00020-1.
[43] T. Kato, S. Hirano, H. Samizo, G. Okada, N. Kawaguchi, K. Shinozaki, H. Masai, T. Yanagida, Dosimetric, luminescence and scintillation properties of Ce-doped CaF2-Al2O3-B2O3 glasses, J. Non-Cryst. Solids 509 (2019) 60–64, https://doi.org/10.1016/j.jnoncrysol.2018.12.025.
[44] N. Wantana, E. Kaewnuam, N. Chanthima, S. Kaewjaeng, H.J. Kim, J. Kaewkhao, Ce3+ doped glass for radiation detection material, Ceram. Int. 44 (2018) S172–S176, https://doi.org/10.1016/j.ceramint.2018.08.121.
[45] H. Masai, G. Okada, A. Torimoto, T. Usui, N. Kawaguchi, T. Yanagida, X-ray-induced scintillation governed by energy transfer process in glasses, Sci. Rep. 8 (2018) 1–8, https://doi.org/10.1038/s41598-017-18954-y.
[46] K. Bartosiewicz, V. Babin, J.A. Mares, A. Beitlerova, Y. Zorenko, A. Iskaliyeva, V. Gorbenko, Z. Bryknar, M. Nikl, Luminescence and energy transfer processes in Ce3+ activated (Gd,Tb)3Al5O12 single crystalline films, J. Lumin. 188 (2017) 60–66, https://doi.org/10.1016/j.jlumin.2017.04.010.
[47] W. Chewpraditkul, K. Wantong, W. Chewpraditkul, N. Yawai, K. Kamada, A. Yoshikawa, M.E. Witkowski, M. Makowski, W. Drozdowski, M. Nikl, Scintillation yield and temperature dependence of radioluminescence of (Lu,Gd)3Al5O12:Ce garnet crystals, Opt. Mater. 120 (2021), https://doi.org/10.1016/j.optmat.2021.111471.
[48] E. Auffray, D. Bouttet, I. Dafinei, J. Fay, P. Lecoq, J.A. Mares, M. Martini, G. Mazé, F. Meinardi, B. Moine, M. Nikl, C. Pedrini, M. Poulain, M. Schneegans, S. Tavernier, A. Vedda, Cerium doped heavy metal fluoride glasses, a possible alternative for electromagnetic calorimetry, Nucl. Instrum. Methods Phys. Res. Sect. A Accel. Spectrom. Detect. Assoc. Equip. (1996) 380, https://doi.org/10.1016/0168-9002(96)00717-6.
[49] H.A. Othman, G.M. Arzumanyan, D. Möncke, The influence of different alkaline earth oxides on the structural and optical properties of undoped, Ce-doped, Sm-doped, and Sm/Ce co-doped lithium alumino-phosphate glasses, Opt. Mater. 62 (2016) 689–696, https://doi.org/10.1016/j.optmat.2016.10.051.
[50] A.V. Ntarisa, S. Saha, P. Aryal, H.J. Kim, A. Khan, N.D. Quang, I.R. Pandey, J. Kaewkhao, S. Kothan, Luminescence and scintillation properties of Ce3+-doped P2O5-Li2CO3-GdBr3-Al2O3 glasses, J. Non-Cryst. Solids 567 (2021), https://doi.org/10.1016/J.JNONCRYSOL.2021.120914, 120914.
[51] N. Wantana, Y. Ruangtaweep, E. Kaewnuam, S. Kothan, H.J. Kim, A. Prasatkhetragarn, J. Kaewkhao, Strong emission from Ce3+ doped gadolinium oxyfluoroborate scintillation glasses matrix, Radiat. Phys. Chem. 185 (2021), https://doi.org/10.1016/j.radphyschem.2021.109497.
[52] E. Elsts, U. Rogulis, K. Bulindzs, K. Smits, A. Zolotarjovs, L. Trinkler, K. Kundzins, Studies of radiation defects in cerium, europium and terbium activated oxyfluoride glasses and glass ceramics, Opt. Mater. 41 (2015) 90–93, https://doi.org/10.1016/j.optmat.2014.10.042.